Laminar Boundary Layer Near the Plane of Symmetry of a Hypersonic Inlet

PAUL A. LIBBY* AND HERBERT FOX†
General Applied Science Laboratories, Inc., Westbury, N. Y.

AND

ROBERT J. SANATOR‡ AND JOSEPH DECARLO§
Republic Aviation Corporation, Farmingdale, N. Y.

The laminar boundary layer in the neighborhood of a centerline of symmetry with adverse pressure gradients and heat transfer is studied with a view toward assessing the importance of three-dimensional effects on such boundary layers in hypersonic inlets. Two approaches are employed. In one, an analysis is performed so that the parameters describing the external flow and the surface geometry are restricted to those yielding similar boundary layers. The numerical results for this analysis are presented for small three-dimensional effects. A second approach is an integral method which can be applied for both similar and nonsimilar flows. The results of both analyses indicate that the boundary-layer thickness can be reduced and separation delayed by spilling the boundary layer away from the centerline of symmetry.

Nomenclature

a_n, b_n, d_n = coefficients in profiles, see Eq. (39)
C = viscosity-density ratio, $\rho\mu/\rho_e\mu_e$
f = modified stream function, see Eqs. (11) and (34)
g = stagnation enthalpy ratio, h_s/h_{se}
h = static enthalpy
h_s = stagnation enthalpy
m = normalizing parameter, see Eqs. (12) and (16)
$\tilde{m}$ = $u_e^2/2h_{se}$ parameter of the external stream
p = pressure
p_2 = curvature of pressure, see Eq. (1)
r = radius of curvature
$\bar{s}$ = transformed x coordinate, see Eq. (10)
u = velocity component in x direction
v = velocity component in y direction, velocity gradient in y direction
w = velocity component in z direction
x,y,z = boundary-layer coordinates, see Fig. 1
X,Y,Z = Cartesian coordinates, see Fig. 1
α = similarity parameter, see Eq. (19)
$\hat{\alpha}$ = $\alpha(1 - \tilde{m})^{-1}$
β = similarity parameter, see Eq. (18)
$\hat{\beta}$ = $\beta(1 - \tilde{m})^{-1}$
γ = similarity parameter, see Eq. (21)
$\hat{\gamma}$ = $\gamma(1 - \tilde{m})^{-1}$
η = transformed normal coordinate, see Eq. (9)
θ = flow deflection
μ = viscosity coefficient
ρ = mass density
σ = Prandtl number
τ = normalized η, η/η_e
$\bar{\varphi}$ = modified stream function, see Eqs. (12, 15, and 35)
φ = $(1 - \tilde{m})\bar{\varphi}$
Φ,Ψ = components of vector stream function, see Eq. (8)
λ = angle of attack (measured in X-Z plane)

Subscripts

e = conditions external to the boundary layer
w = conditions at the body surface
∞ = conditions in the undistributed stream
0,1,2 = terms in expansions, see Eqs. (1) and (28)

Presented at the AIAA-ASME Hypersonic Ramjet Conference, White Oak, Md., April 23–25, 1963; revision received September 26, 1963. The General Applied Science Laboratories' effort connected with the research reported here was sponsored by Republic Aviation Corporation under letter agreement dated August 1, 1962. The authors are pleased to acknowledge that Antonio Ferri suggested this investigation and that Lu Ting provided helpful discussion. Special credit is due M. Gershinsky, Saul Serben, Georgia Wenderoth, and Rochelle Kellman of the Digital Programming and Mathematical Analysis Section, Republic Aviation Corporation, for their assistance in the numerical solutions of the boundary-layer equations.

* Senior Scientific Investigator; also Professor of Aerospace Engineering, Polytechnic Institute of Brooklyn, Freeport, N. Y. Member AIAA.

† Formerly Scientific Specialist; presently Research Associate, Department of Aerospace Engineering and Applied Mechanics, Polytechnic Institute of Brooklyn, Freeport, N. Y. Member AIAA.

‡ Assistant Project Manager in charge of Fluid Mechanics, Advanced Aircraft and Vehicles Division. Member AIAA.

§ Senior Aerodynamicist, Advanced Aircraft and Vehicle Division.

Introduction

THE boundary layer in the most general case of three-dimensional flow cannot be analyzed except by cumbersome numerical methods. However, three-dimensional effects play an important role in many flows of practical interest. In recent years this conflict between complexity and importance has been partially resolved by considering rather idealized three-dimensional flows and by hoping that the resultant studies might shed light on the main features of three-dimensionality.

Review of Previous Research

The literature on such idealized three-dimensional flows is extensive; it was reviewed in 1956 by Moore[1] and more recently (1960) by Cooke and Hall.[2] Of particular interest to the present report are the three-dimensional effects which may arise on the inlets of hypersonic air-breathing vehicles. The boundary layers on such inlets involve adverse pressure gradients, hypersonic flow external to the boundary layer, and high rates of heat transfer. Laminar or turbulent flow may prevail, although, at high altitudes and either for small vehicles or on components of large vehicles, laminar flow is likely to prevail.

Three-dimensional effects on boundary-layer behavior may be important in inlets for several reasons. First, the performance of the inlet can be significantly degraded by thick boundary layers and by boundary-layer separation. By introducing small cross-flows to an essentially two-dimen-

sional or axisymmetric inlet, it may be possible to reduce significantly the thickness of the boundary layer entering the combustor, and either to prevent or to reduce flow separation. This corresponds to employing three-dimensional effects as boundary-layer control. Second, the over-all configuration of the inlet may be such as to result in three-dimensional boundary layers.

The analysis of compressible three-dimensional flows with heat transfer and with either laminar or turbulent transport has not received extensive consideration. In the most closely related studies, Wilkinson[3] and Moore[4] treated the incompressible flow along a flat surface in the neighborhood of a plane of symmetry with wedge-type flow in the direction of the main stream. Johnston[5] treated the incompressible turbulent flow along a plane of symmetry. The yawed, infinite cylinder has been the subject of considerable research for laminar flow[6-8] and of limited research for turbulent incompressible flow.[9,10,20]

In this report the laminar flow along a centerline of symmetry is treated; primary emphasis is devoted to flows with adverse pressure gradient and heat transfer. An analysis of similiar flows is carried out first; it is shown that the usual similarity restrictions arising in two-dimensional or axisymmetric flows are supplemented by additional restrictions due to three-dimensionality. Indeed, for streamwise pressure gradient the limiting case of infinite external Mach number must be considered. It is shown that for these flows the velocity profiles for the cross-flow involve large velocity overshoot.

The describing equations for this case involve three coupled, nonlinear ordinary differential equations with split boundary conditions. Presented here are solutions for the linearized cases of small cross-flow only, either out of or into the plane of symmetry.

Also presented is a second analysis which will yield approximate results for more general, i.e., nonsimilar, flows; it is based on an integral method in terms of the similarity variable η. Thus, approximate solutions for similar flows with large three-dimensional effects and for nonsimilar flows can be obtained. The results of the two analyses are compared when possible, and the implications of the analyses with respect to the boundary layer on a hypersonic inlet are discussed.

Analysis

In Fig. 1 the coordinate system and schematic representation of the flow in the neighborhood of a plane of symmetry are shown. The coordinate system is that suggested by Moore[1] in that only one scalar is introduced. The present application involves the x-z plane as the plane of symmetry. Note that, if the surface is flat, the coordinate y should be considered the Cartesian coordinate normal to the x-z plane

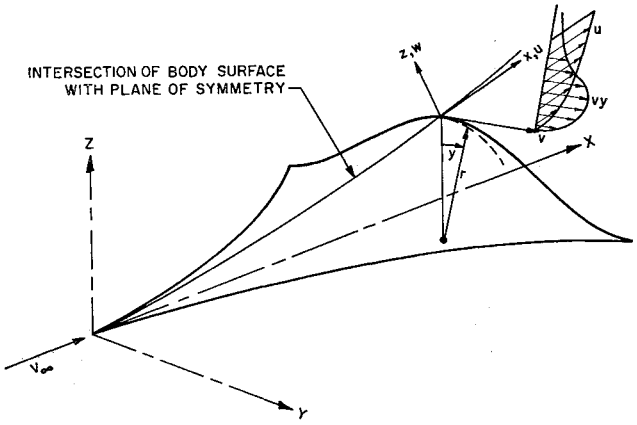

Fig. 1 Schematic representation of flow and coordinate system.

and the scalar r becomes unity, whereas on a curved surface these quantities are, respectively, an angle and a radius of curvature. The main discussion presented below will assume that with proper interpretation the analysis applies to flat surfaces with three-dimensional effects imposed by the external flow as, for example, from an interfering external surface. It should also be noted that the scalar r has been taken here in the plane normal to the X axis so that the angle y, defining a generic point in the neighborhood of the centerline of symmetry, is measured in that plane. This selection facilitates reduction to the axisymmetric case. However, for an axisymmetric body at an angle of attack, it may be more convenient to measure r in a plane normal to the body axis.

General Equations

Consider an expansion of the flow and geometric quantities suggested by symmetry; thus, let

$$\begin{aligned} u(x,y,z) &= u_0(x,z) + y^2u_2(x,z) + \dots \\ w(x,y,z) &= w_0(x,z) + y^2w_2(x,z) + \dots \\ v(x,y,z) &= yv_1(x,z) + y^3v_3(x,z) + \dots \\ p(x,y) &= p_0(x) + y^2p_2(x) + \dots \\ r(x,y) &= r_0(x) + y^2r_2(x) + \dots \\ \rho(x,y,z) &= \rho_0(x,z) + y^2\rho_2(x,z) + \dots \\ h_s(x,y,z) &= h_{s0}(x,z) + y^2h_{s2}(x,z) + \dots \end{aligned} \tag{1}$$

Substitution of Eqs. (1) into the boundary-layer equations of Ref. 1 and collection of terms in powers of y results, to the first order in y, in the following:

x-Directional Momentum

$$\rho uu_x + \rho wu_z = -(p)_x + (\mu u_z)_z \tag{2}$$

y-Directional Momentum

$$\rho u(rv)_x + \rho(rv)^2/r^2 + \rho w(rv)_z = -2p_2 + [\mu(vr)_z]_z \tag{3}$$

Continuity

$$(\rho ru)_x + \rho v + r(\rho w)_z = 0 \tag{4}$$

Energy

$$\rho u(h_s)x + \rho w(h_s)_z = [(\mu/\sigma)(h_s)_z + (1 - \sigma^{-1})\mu uu_z]_z \tag{5}$$

where the subscripts denoting the order of the terms have been dropped when possible in the interest of simplicity. All quantities retain their usual physical significance with the exception of v (which must be interpreted as proportional to the velocity gradient in the direction normal to the plane of symmetry) and of p_2 (which is proportional to the curvature of the pressure distribution along the plane of symmetry). These equations plus the appropriate boundary conditions at $z = 0, \infty$ define u, v, w, ρ, h_s as functions of x and z provided that certain auxiliary functions are available. These are p, p_2, and r as functions of x; μ and σ, for example, as functions of the static enthalpy h; and an equation of state taken here in the form $\rho \sim h^{-1}$. The boundary conditions at $z = 0$ are $u = v = w = 0, h_s = h_w$; and at $z \to \infty$ they are $u = u_e, v = v_e, h = h_{se}$. The functions u_e and v_e are related to the quantities p, p_2, and r by Eqs. (2) and (3) applied as $z \to \infty$, namely,

$$\rho_e u_e(u_e)_x = -p_x \tag{6}$$

and

$$\rho_e u_e(rv_e)_x + \rho_e v_e^2 = -2p_2 \tag{7}$$

Equations for Similar Flows

The simplification associated with similarity of the boundary layer has been found in recent years to yield instructive

results in many cases; as might be expected, in the flow under consideration certain variations of p, p_2, and r are required for similarity. The approach employed here utilizes the vector stream function used previously in three-dimensional boundary-layer theory[1] and the Levy-Lees transformation[11,12] used extensively in two-dimensional and axisymmetric flows and by Vaglio-Laurin[13] for three-dimensional flows in terms of streamline coordinates.

Equation (4) is satisfied by arbitrary functions Ψ and Φ related to the velocity components u, v, w by

$$\begin{aligned} \rho r u &= \Psi_z \\ \rho v &= \Phi_z \\ \rho w r &= -\Psi_x - \Phi \end{aligned} \tag{8}$$

Now introduce the new independent variables η and $\tilde{s}$ defined by

$$\eta \equiv \rho_e u_e r (2\tilde{s})^{-1/2} \int_0^z \left(\frac{\rho}{\rho_e}\right) dz = \eta(x,z) \tag{9}$$

$$\tilde{s} = \int_0^x \rho_e \mu_e r^2 dx = \tilde{s}(x) \tag{10}$$

and seek similar solutions so that

$$\Psi = (2\tilde{s})^{1/2} f(\eta) \tag{11}$$

$$\Phi = m(\tilde{s})\,\bar{\varphi}(\eta) \tag{12}$$

where $m(\tilde{s})$ will be determined by normalization of the cross-flow velocity profile v/v_e. The differential operators required for the transformation of the equations from $x, z \rightarrow \eta, \tilde{s}$ are

$$\begin{aligned} \frac{\partial}{\partial x} &= \frac{d\tilde{s}}{dx}\frac{\partial}{\partial \tilde{s}} + \left(\frac{\partial \eta}{\partial x}\right)\frac{\partial}{\partial \eta} \\ \frac{\partial}{\partial z} &= \rho u_e r (2\tilde{s})^{-1/2}\frac{\partial}{\partial \eta} \end{aligned} \tag{13}$$

Application of Eqs. (13) permits Eqs. (8) to be used to show that

$$f' = u/u_e \tag{14}$$

and

$$\bar{\varphi}' = v/v_e \tag{15}$$

where $(\;)'$ denotes $d/d\eta$, provided

$$[u_e r m/(2\tilde{s})^{1/2} v_e] = 1 \tag{16}$$

Equation (16) is considered to define m in terms of the external flow and geometric properties.

If, as is customary in similarity analyses, Eq. (2) is transformed by application of Eq. (13) to an ordinary differential equation in η, there is obtained

$$(Cf'')' + f''(f + \alpha\bar{\varphi}) + \beta[(\rho_e/\rho) - f'^2] = 0 \tag{17}$$

where

$$\beta \equiv (2\tilde{s}/u_e)(du_e/d\tilde{s}) \tag{18}$$

and

$$\alpha \equiv m(2\tilde{s})^{1/2}/\rho_e \mu_e u_e r^2 \tag{19}$$

or from Eq. (16)

$$\alpha = 2\tilde{s} v_e/\rho_e \mu_e u_e^2 r^3 \tag{19a}$$

For similarity α and β must be constants and C and ρ_e/ρ must be functions of η alone. Note that β is the usual similarity parameter for two-dimensional or axisymmetric flows and that $\alpha > 0$ for outflow from the plane of symmetry.

Similarly, Eq. (3) becomes

$$\begin{aligned} (C\bar{\varphi}'')' + f\bar{\varphi}'' + \alpha[(\rho_e/\rho) - \varphi'^2 + \bar{\varphi}\bar{\varphi}''] + \\ \gamma[(\rho_e/\rho) - f'\bar{\varphi}'] = 0 \end{aligned} \tag{20}$$

where the additional similarity parameter which must be constant for similar flows is

$$\gamma \equiv (2\tilde{s}/rv_e)[d(rv_e)/d\tilde{s}] \tag{21}$$

Finally, the energy equation, Eq. (5), becomes, for a constant Prandtl number σ,

$$(Cg')' + g'(f + \alpha\bar{\varphi})\sigma + 2\tilde{m}(\sigma - 1)(Cf'f'')' = 0 \tag{22}$$

where $g \equiv h_s/h_{se}$ and where $\tilde{m} = (u_e^2/2h_{se})$ is an external stream parameter which must be constant for similar flows.

It will be convenient for further discussion to introduce the approximate equation of state:

$$\rho_e/\rho \simeq h/h_e \tag{23}$$

Then the definitions of stagnation enthalpy and of g permit development of the expression

$$\rho_e/\rho = (g - \tilde{m}f'^2)/(1 - \tilde{m}) \tag{24}$$

Substitution of Eq. (24) into Eqs. (17) and (20) results in

$$(Cf'') + f''(f + \alpha\bar{\varphi}) + \hat{\beta}\,(g - f'^2) = 0 \tag{17a}$$

$$\begin{aligned} (C\bar{\varphi}'')' + f\bar{\varphi}'' + \hat{\gamma}[g - \bar{\varphi}'f' + \tilde{m}(f'\bar{\varphi}' - f'^2)] + \\ \hat{\alpha}[g + \bar{\varphi}\bar{\varphi}'' - \bar{\varphi}'^2 + \tilde{m}(\varphi'^2 - \bar{\varphi}\bar{\varphi}'' - f'^2)] = 0 \end{aligned} \tag{20a}$$

where $\hat{\beta} \equiv \beta/(1 - \tilde{m})$, $\hat{\gamma} = \gamma/(1 - \tilde{m})$, $\hat{\alpha} = \alpha/(1 - \tilde{m})$. Note that both α and $\hat{\alpha}$ appear; this will be significant in the later discussion.

Remarks on the Similarity Conditions and the Final Equations

At this point in the analysis it is interesting to consider some of the implications of the similarity restrictions. First, for axisymmetric flow, i.e., $\alpha, \hat{\alpha}, \hat{\gamma} = 0$, the usual similarity requirements prevail. These have been discussed in detail in Refs. 11 and 12, for example, and can be summarized briefly here. Require that C and ρ_e/ρ be expressed in terms of the static enthalpy ratio h/h_e and that g_w be constant. Then the axisymmetric flow will be similar provided that either

$$\hat{\beta} = 0 \tag{i}$$

or that for $\sigma \neq 1$

$$\tilde{m} \ll 1 \text{ and } \hat{\beta} = \text{const} \tag{ii}$$

or that for $\sigma \neq 1$

$$m \simeq 1 \text{ and } \hat{\beta} = \text{const} \tag{iii}$$

or that for $\sigma = 1$

$$\hat{\beta} = \text{const} \tag{iv}$$

For application to problems connected with inlets of air-breathing hypersonic vehicles, the cases $\tilde{m} \simeq 1$, $\hat{\beta} = \text{const} \neq 0$ [i.e., either (iii) or (iv)] are of most interest; in these cases $\beta \rightarrow 0$, but $\hat{\beta}$ is finite and constant for similar flows. It should be noted that this hypersonic case, $\tilde{m} \simeq 1$, $\hat{\beta} \neq 0$, corresponds to only approximate similarity in the limiting sense of $\tilde{m} \rightarrow 1$. The equations which result for this case should really be considered the first-order equations in a power-series expansion in $1 - \tilde{m}_0 \ll 1$, where $\tilde{m}_0$ is a constant, reference value for $\tilde{m}$, e.g., $\tilde{m}_\infty$. The equations for the higher-order solutions would be linear partial differential equations, i.e., they would involve both η and $\tilde{s}$ as independent variables.

Now for flows with a three-dimensional component, i.e., $\hat{\alpha}, \alpha, \hat{\gamma} \neq 0$, the forementioned requirements for flow similarity are supplemented by making these additional parameters constant and thus by imposing restrictions on v_e and r. However, the appearance of $\tilde{m}$ in Eq. (20a) implies that the usual simplification $\sigma = 1$ is not sufficient in this case. Clearly, if $\tilde{m} \ll 1$, i.e., if case (ii) prevails, $\tilde{m}$ disappears from Eq. (20a), and similarity is assured. At the other limit, namely, the one of interest herein, $\tilde{m} \simeq 1$, it is necessary to consider a special treatment for similar flows and to

let $\alpha \to 0$, i.e., $v_e \to 0$ and $\bar{\varphi} \to \infty$. This limiting behavior is necessary in order to preserve a three-dimensional effect in the describing equations, since, if α remains finite, Eqs. (17) and (22) along with Eq. (24) become those applicable to axisymmetric flows. Thus, define $\varphi = (1 - \tilde{m})\bar{\varphi}$ so that $\alpha\bar{\varphi} = \hat{\alpha}\varphi$. It will be shown below that $\varphi(\eta)$ yields a physically satisfactory profile for the cross-flow velocity.

In terms of φ, Eqs. (17a, 20a, and 22) become, for general $\tilde{m}$,

$$(Cf'')' + f''(f + \hat{\alpha}\varphi) + \hat{\beta}(g - f'^2) = 0 \qquad (17b)$$

$$(C\varphi'')' + \varphi''f + \gamma(g - \tilde{m}f'^2 - \varphi'f') + \hat{\alpha}[(g - \tilde{m}f'^2)(1 - \tilde{m}) + \varphi\varphi'' - \varphi'^2)] = 0 \qquad (20b)$$

$$(Cg')' + g'(f + \hat{\alpha}\varphi)\sigma + 2\tilde{m}(\sigma - 1)(Cf'f'')' = 0 \qquad (22a)$$

Clearly, no change has been made for the case $\tilde{m} \ll 1$, but for $\tilde{m} \to 1$, Eqs. (20b) and (22a) become

$$(C\varphi'')' + \varphi''f + \gamma(g - f'^2 - \varphi'f') + \hat{\alpha}(\varphi\varphi'' - \varphi'^2) = 0 \qquad (20c)$$

$$(Cg')' + g'(f + \hat{\alpha}\varphi)\sigma + 2(\sigma - 1)(Cf'f'')' = 0 \qquad (22b)$$

Equations (17b, 20c, and 22b) represent the final equations for $\tilde{m} \simeq 1$, and imply that the similarity requirements are $\hat{\alpha},\hat{\beta},\gamma = \text{const}$.

It is of interest to consider the velocity profile for the cross-flow in order to see if a physically satisfactory flow is described by this limiting process. From Eq. (15) and the definition of φ there is obtained

$$\varphi' = v(1 - \tilde{m})/v_e \qquad (15a)$$

or in terms of $\hat{\alpha}$

$$\varphi' = v[2\tilde{s}/\hat{\alpha}\rho_e\mu_e u_e^2 r^3] \qquad (15b)$$

Note that φ' is well defined for finite $\hat{\alpha}$, that no difficulty is introduced by consideration of $\tilde{m} \simeq 1$, and that $v_e(1 - \tilde{m})^{-1}$ is finite as $\tilde{m} \to 1$. However, the boundary condition on φ' as $\eta \to \infty$ is altered by this limiting process from that which might be casually expected; from Eq. (15a) note that, as $\eta \to \infty$, $v/v_e \to 1$ (both v and $v_e \to 0$) so that $\varphi' \to 0$ as $\tilde{m} \to 1$. Since within the boundary layer it is expected that $\varphi' \not\equiv 0$, it may be concluded that, for the case of hypersonic Mach numbers external to the boundary layer, large (indeed infinite) velocity overshoot occurs.‖ Physically this is reasonable if it is recalled that within a hypersonic boundary layer the density is small compared to that in the external stream. Thus, if a boundary layer is subjected to crosswise forces due to a curvature of pressure, i.e., due to $p_2 \neq 0$, the gas within the layer responds and moves laterally, whereas the gas in the external stream and at the surface is unable to do so. This situation should be compared to the case of three-dimensional flow with low external Mach number and with a "cold-wall"; in this case, treated in Ref. 13, the cross-flow is negligible. Large cross-flow overshoot has been previously demonstrated for conical flow ($\hat{\beta} = 0$) (see, e.g., Ref. 14).

The remaining boundary conditions in f, g, and φ are also of interest; at $\eta \to \infty$ it is clear that $f' = 1$, $g = 1$. On the surface $\eta = 0$, $f' = 0$, $\varphi' = 0$, $g = g_w$, and since $w = 0$, there is obtained, after some rearrangement from Eqs. (8, 11–13, 19a) and from the equation $\alpha\bar{\varphi} = \hat{\alpha}\varphi$, the condition $f + \hat{\alpha}\varphi = 0$ at $\eta = 0$. It should be noted that, because f and φ appear in the describing equations, e.g., Eqs. (17b, 20b, and 22a), only as $(f + \alpha\varphi)$, arbitrary constants can be added to f and φ provided that this last condition is satisfied; thus it is permissible to take $f = \varphi = 0$ at $\eta = 0$.

‖ Note that the actual magnitude of the velocity ratio, yv_e/u_e, will depend on the properties of the three-dimensional inviscid flow and on the distance from the plane of symmetry and may be relatively small compared to unity.

It is also of interest to note that γ rather than $\hat{\gamma}$ remains in the final equations; from the definitions of γ and $\tilde{m}$ it is easy to show that

$$\gamma = 2\tilde{s}[rv_e/(1 - \tilde{m})]^{-1}(d/d\tilde{s})[rv_e/(1 - \tilde{m})] - 2\tilde{m}\hat{\beta} \qquad (25)$$

which also is well behaved as $\tilde{m} \to 1$, provided that $v_e(1 - \tilde{m})^{-1}$ is finite.

As in all analyses of similar flows involving several similarity parameters, it is possible to take a variety of points of view relating particular values of these parameters to physical flows. Herein it has been found useful to adopt the following considerations. Two general classes of body shapes are treated: those whose radius r increases linearly with x, and those whose radius r is constant. From the definition of the transformation $\tilde{s} = \tilde{s}(x)$, it may be seen that, for hypersonic flow, i.e., $u_e \simeq \text{const}$, and for $\rho_e\mu_e \simeq \text{const}$, the first class of bodies implies roughly $r \sim \tilde{s}^{1/3}$; on the contrary, the second class implies $r \sim \tilde{s}^0$. Both classes may be treated by letting $r \sim \tilde{s}^{k_1}$. With the geometry specified in this general way, it is next considered that the value of $\hat{\beta}$, identifying a particular pressure distribution in this external flow, is chosen. It will now be shown that the value of γ is no longer arbitrary, although the value of $\hat{\alpha}$ is Eq. (19a) plus the relation $\hat{\alpha} \equiv \alpha(1 - \tilde{m})^{-1}$ leads to

$$\hat{\alpha} = [2\tilde{s}/\rho_e\mu_e u_e^2 r^4][rv_e/(1 - \tilde{m})] \qquad (19b)$$

Introduce a function of $\tilde{s}$, namely, $G(\tilde{s}) \equiv \rho_e\mu_e u_e^2 r^4/2\tilde{s}$. Then $[rv_e/(1 - \tilde{m})] = \hat{\alpha}G$, and since $\hat{\alpha} = \text{const}$, Eq. (25) becomes an equation for $G(\tilde{s})$, namely,

$$(2\tilde{s}/G)dG/d\tilde{s} = \gamma + 2\tilde{m}\hat{\beta} \simeq \gamma + 2\hat{\beta}$$

whose solution is

$$G \sim \tilde{s}^{(\gamma/2)+\beta} \qquad (26)$$

Again consider $\rho_e\mu_e u_e^2$ roughly constant so that Eq. (26) plus the relation $r \sim \tilde{s}^{k_1}$ implies

$$\gamma = 8k_1 - 2\hat{\beta} - 2 \qquad (27)$$

Equation (27) relates, then, the parameter specifying the external flow $\hat{\beta}$ and a rough geometric parameter k_1 whose value here is taken to be either $\frac{1}{3}$ or zero. If $\hat{\beta} = 0$ and $k_1 = \frac{1}{3}$, i.e., if the flow about a cone is considered, then from Eq. (27), $\gamma = \frac{2}{3}$, which is in agreement with previous work (see, for example, Ref. 1). Also, for this special case, the describing equations derived here are in accord with previous studies (see Refs. 1 and 14).#

Discussion of the Final Equations

The final equations describing the flow of interest in hypersonic inlets, i.e., Eqs. (17b, 20c, and 22b), must be supplemented by a representation of C in terms of g and f', by a value for σ, and by values for the parameters $\hat{\alpha}$, γ, $\hat{\beta}$, and g_w. The eigenvalues of the problem f_w'',g_w', and φ_w'' must be found by trial-and-error integration starting from the surface ($\eta = 0$) as in Refs. 14 and 16 or from the asymptotic solution valid as $\eta \to \infty$ as in Refs. 17–19. Even for the case of $C \equiv 1$, the task would be considerable; however, first-order effects of three-dimensionality can be obtained after Moore,[4] by taking $\hat{\alpha}$ to be small and by letting

$$\begin{aligned} f &= f_0 + \hat{\alpha}f_1 + \hat{\alpha}^2 f_2 + \\ \varphi &= \varphi_0 + \hat{\alpha}\varphi_1 + \hat{\alpha}^2\varphi_2 + \\ g &= g_0 + \hat{\alpha}g_1 + \hat{\alpha}^2 g_2 + \end{aligned} \qquad (28)$$

It may be of interest to note here that in Ref. 15 a Newtonian flow theory is applied to relate p and p_2 to surface geometry under the assumption, of course, that the pressure distribution is due only to surface geometry. It is found that only in the case $\hat{\beta} = 0$, i.e., in the flow over a cone, are the similarity requirements compatible with a Newtonian pressure distribution.

Then the equations for f_0 and g_0 would be those for axisymmetric or two-dimensional flow, i.e., for $C = 1$ and $\sigma = 1$,

$$f_0''' + f_0 f_0'' + \hat{\beta}(g_0 - f_0'^2) = 0 \tag{29}$$

$$g_0'' + f_0 g_0' = 0 \tag{30}$$

whereas the equation for φ_0 would be linear with variable coefficients, namely,

$$\varphi_0''' + \varphi_0'' f_0 + \gamma(g_0 - f_0'^2 - \varphi_0' f_0') = 0 \tag{31}$$

The solution of Eqs. (29) and (30) for various values of g_w and $\hat{\beta}$ has been given by Cohen and Reshotko.[16] Note that the boundary conditions on the zero-order solutions at $\eta = 0$ are $f_0 = f_0' = \varphi_0 = \varphi_0' = 0$, $g_0 = g_{0w}$; and at $\eta \to \infty$ they are $f_0' = g_0 = 1$, $\varphi_0' = 0$. The solution of Eq. (31) must be carried out numerically.

The first-order effect of cross-flow will be given by solution of the equations for f_1 and g_1, namely, by

$$f_1''' + f_0 f_1'' + \hat{\beta}(g_1 - 2f_0' f_1') + f_0'' f_1 = -\varphi_0 f_0'' \tag{32}$$

$$g_1'' + f_0 g_1' + g_0' f_1 = -g_0' \varphi_0 \tag{33}$$

The boundary conditions are homogeneous, namely, $f_1(0) = f_1'(0) = g_1(0) = f_1'(\infty) = g_1(\infty) = 0$. These are linear equations with variable coefficients; the eigenvalues $f_1''(0)$, $g_1'(0)$ making $f_1'(\infty)$, $g_1(\infty) = 0$ can be found numerically.

Of particular concern for application of these equations to the hypersonic inlet problem will be cases of $\hat{\beta} < 0$, $\hat{\alpha} > 0$, and the effect of $\hat{\alpha}$ on skin friction and heat transfer. Thus, $f_w'' = f_0''(0) + \hat{\alpha} f_1''(0)$ and $g_w' = g_0'(0) + \hat{\alpha} g_1'(0)$ will be of interest; for example, if $f_0''(0)$ is small, i.e., the zero-order flow is close to separation, it would be expected on physical grounds that for $\hat{\alpha} > 0$ (outflow from the plane of symmetry) the wall shear would be increased, i.e., separation would be delayed. These considerations for incompressible flow were made in Refs. 3 and 4. (It will be recognized that the present analysis can be applied directly to flows which involve $\hat{\beta} > 0$, $\hat{\alpha} > 0$ and which correspond to the windward side of lifting slender bodies.)

An Integral Method

For boundary-layer flows of the nonsimilar type, either large-scale numerical methods (which are in principle exact) or approximate methods are required. In this section an approximate method based on the well-known integral approach is developed; however, in line with recent developments in boundary-layer theory, the integral method utilizing the similarity variables η and $\tilde{s}$ is employed. This variation of the usual integral method was apparently first suggested by Hayes[21] (see also Hayes and Probstein[12] for two-dimensional and axisymmetric flows) and has the advantage of providing a unified description of nonsimilar and similar flows; i.e., for nonsimilar cases, the integral method yields a set of ordinary differential equations with $\tilde{s}$ as the independent variable, and for similar cases a corresponding set of algebraic equations is obtained by setting $d/d\tilde{s} \equiv 0$. It is noted that in nonsimilar flows of interest, namely those with $\hat{\beta} < 0$, $\hat{\alpha} > 0$, the restrictions on $\hat{\beta}$, $\hat{\alpha}$, γ, and in particular on $\tilde{m}$ are not required.

To approach nonsimilar flows for the present problem of the boundary layer in the neighborhood of the centerline of symmetry, it is first necessary to generalize Eqs. (11) and (12), i.e., those for the vector stream function, according to

$$\Psi = (2\tilde{s})^{1/2} f(\tilde{s},\eta) \tag{34}$$

$$\Phi = m(\tilde{s})\,\bar{\varphi}(\tilde{s},\eta) \tag{35}$$

where $m(\tilde{s})$ is again defined by Eq. (16) and is a known function of external flow and geometric properties. If the transformations of Eqs. (9) and (10) are applied to the general conservation equations, i.e., to Eqs. (2–5), there are obtained

$$(Cf'')' + ff'' + \beta\left[\frac{\rho_e}{\rho} - f'^2\right] + \alpha\bar{\varphi}f'' = 2\tilde{s}\left[f'\frac{\partial f'}{\partial \tilde{s}} - \frac{\partial f}{\partial \tilde{s}}f''\right] \tag{36}$$

$$(C\varphi'')' + f\varphi'' + \gamma\left[\frac{\rho_e}{\rho} - f'\bar{\varphi}'\right] + \alpha\left[\frac{\rho_e}{\rho} + \bar{\varphi}\bar{\varphi}'' - \varphi'^2\right] = 2\tilde{s}\left[f'\frac{\partial \bar{\varphi}}{\partial \tilde{s}} - \frac{\partial f}{\partial \tilde{s}}\bar{\varphi}''\right] \tag{37}$$

$$\left(\frac{C}{\sigma}g'\right)' + g'(f + \alpha\bar{\varphi}) + 2\tilde{m}\left[C\left(1 - \frac{1}{\sigma}\right)f'f''\right]' = 2\tilde{s}\left[f'\frac{\partial g}{\partial \tilde{s}} - \frac{\partial f}{\partial \tilde{s}}g'\right] \tag{38}$$

where, in general, C, β, α, γ, σ, and $\tilde{m}$ are functions of $\tilde{s}$ and η and where $(\;)'$ in this more general case denotes partial differentiation with respect to η. Employ again an approximate equation of state $\rho_e/\rho \simeq h/h_e$ so that Eq. (24) applies.

Conventional integral conditions may now be developed by multiplying Eqs. (36–38) by $d\eta$ and by integrating from zero to an "edge" denoted by η_e.** Profiles for f', φ', and g are assumed as polynomials in $\tau \equiv \eta/\eta_e$ according to

$$\left.\begin{aligned} f' &= \sum_{n=0}^{4} a_n \tau^n \\ \bar{\varphi}' &= \sum_{n=0}^{5} d_n \tau^n \\ g &= \sum_{n=0}^{5} b_n \tau^n \end{aligned}\right\} \tag{39}$$

where the coefficients a_n, b_n, d_n are selected so that

$$\left.\begin{aligned} &\text{at } \tau = 0\text{:}\quad f' = \bar{\varphi}' = 0;\ g = g_w \\ &\text{at } \tau = 1\text{:}\quad f' = \bar{\varphi}' = g = 1 \\ &\qquad\qquad f'' = \bar{\varphi}'' = g' = 0 \\ &\qquad\qquad f''' = \bar{\varphi}''' = g'' = 0 \end{aligned}\right\} \tag{40}$$

Note that these conditions leave one free parameter for f' and two free parameters each for $\bar{\varphi}'$ and g; herein these parameters are taken to be a_2, b_1, b_2, d_2, and d_5. In general, these free coefficients are to be regarded as functions of $\tilde{s}$.

Now consider the mathematical situation at this point. The view taken herein is that the integral conditions represent three equations in the following unknown functions of $\tilde{s}$: $\eta_e, a_2, b_1, d_2, d_5, b_2$. It is assumed that the following parameters defining the external flow and the surface geometry are specified in general as functions of $\tilde{s}$: $g_w, C_w, \alpha, \hat{\beta}, \hat{\gamma}, \hat{\alpha}, \tilde{m}, \sigma_w$. (Note that as in any conventional integral method only the transport properties at the surface, i.e., only C_w and σ_w, appear.) Clearly then, three additional equations are required; after the usual integral method, these are obtained by selecting a_2, d_2, and b_2 so that the profiles satisfy the exact equations at the surface, i.e., Eqs. (36–38) evaluated at $\eta = 0$. There results

$$\left.\begin{aligned} a_2 &= -\hat{\beta} g_w \eta_e^2/2C_w \\ d_2 &= -(\hat{\gamma} + \hat{\alpha}) g_w \eta_e^2/2C_w \\ b_2 &= -\tilde{m}(\sigma_w - 1)\left[2 + \frac{\hat{\beta}}{6}\frac{g_w}{C_w}\eta_e^2\right]^2 \end{aligned}\right\} \tag{41}$$

** Note that in the present report only a simple averaging over η is used; clearly multiple integral methods involving multiplication by $\eta^m u^n d\eta$ prior to integration can be developed so that there could be employed an approach due to Tani[22] which frees the wall properties of the profiles from local freestream conditions, and which would provide greater accuracy, especially for adverse gradients.

Thus the integral conditions and Eq. (41) permit the previously listed six unknowns to be determined as functions of $\tilde{s}$; the mathematical problem is characterized as involving three, first-order, nonlinear ordinary differential equations and three algebraic equations. The integration may be carried out by standard techniques with a small-scale computer being adequate. There are three initial conditions to be specified. In general, with the variation of the integral method employed here, the solution starts from a similar solution applicable as $\tilde{s} \to 0$; i.e., the parameters specifying the external flow and surface geometry must approach constant values as $\tilde{s} \to 0$. Algebraic equations defining the initial values of $\eta_e, \ldots b_2$ result. The solution thereof would prevail for increasing $\tilde{s}$ until significant nonsimilar changes in one of the parameters defining the external flow or the surface geometry occur.

Of particular interest from a solution given by the integral method will be the shear parameters f_w'' and the heat-transfer parameter g_w'; these will be given as functions of $\tilde{s}$ according to

$$f_w'' = a_1/\eta_e \qquad g_w' = b_1/\eta_e \tag{42}$$

It is perhaps worth noting that, if the integral method is applied to flows corresponding to $\hat{\alpha} \neq 0$ and to $\tilde{m} \to 1$, it would be expected from the similarity analysis just presented that large crosswise velocity overshoot would be expected, i.e., that $(\bar{\varphi}')_{max} \gg 1$. The assumed profile for $\bar{\varphi}'$ with the parameters d_2 and d_5 permits such overshoot.

Numerical Solutions

The governing equations, subject to surface and stream boundary conditions, were solved numerically for a variety of cases using the Republic IBM 7090 digital computer. Two separate and distinct programs were designed, one for the similar solutions, and one for the nonsimilar solutions using the previously described integral method.

1. *Similar solutions*

The mathematical statement of the problem consists of the system of linear second- and third-order differential equations given by Eqs. (31–33) with their associated boundary conditions. Equation (31) can be reduced to one involving the second derivative of the cross-flow velocity function as the highest-order derivative by introducing $\Phi_0 = \varphi'$ and replacing, in Eqs. (32) and (33), the function φ_0 by

$$\int_0^\eta \Phi_0(\xi)d\xi$$

where ξ is a dummy variable of integration.

The second-order equation for Φ_0 can be solved numerically in terms of two first-order equations with f_0, f_0', and g_0' provided by Ref. 16; two solutions, one to the homogeneous equations and one to the inhomogeneous equations, are combined so that Φ_0 approaches zero as $\eta \to \infty$. The solution for Φ_0 provides the inhomogeneous terms in Eqs. (32) and (33) which must be solved simultaneously and which are rewritten as five, first-order, linear ordinary differential equations in order to employ usual integration techniques. It is possible to combine two independent numerical solutions to the homogeneous equations with one solution of the inhomogeneous set so that the boundary conditions at $\eta \to \infty$ are satisfied.

2. *Integral method*

The set of three differential and three algebraic equations arising in the integral method is solved by standard integration techniques employed for $\tilde{s} > 0$.†† By elimination, three differential equations, e.g., for η_e, b_1, and d_5, result. In lieu of deriving the starting values for the integration directly from the three algebraic equations, the values prevailing as $\tilde{s} \to 0$ are obtained from the same integration program as follows:

1) The values of g_w, $\hat{\beta}$, $\hat{\alpha}$, γ, and $\tilde{m}$ prevailing at $\tilde{s} = 0$ are inserted in the differential equations as constant values.

2) At an arbitrarily selected positive value of $\tilde{s}$ near zero, initial values of η_e, b_1, and d_5, considered to be first approximations to the values prevailing at $\tilde{s} = 0$, are imposed.

3) The integration is carried out for increasing $\tilde{s}$ until the quantities $|\tilde{s}(d\eta_e/d\tilde{s})|$, $|\tilde{s}(db_1/d\tilde{s})|$, and $|\tilde{s}(dd_5/d\tilde{s})|$ become negligibly small. The values of η_e, b_1, and d_5 which result are those corresponding to the similar flow prevailing at $\tilde{s} = 0$. (Reference 23 provides details of the integral method and of the numerical analysis.)

Table 1 Similar solutions

Case	$\hat{\beta}$	g_w	k_1	Remark
1	−0.1295	2.0	$\frac{1}{3}$, 0	separation profile
2	−0.2	0.6	$\frac{1}{3}$, 0	
3	−0.24	0.6	$\frac{1}{3}$, 0	incipient separation
4	−0.3	0.2	$\frac{1}{3}$	
5	−0.325	0.2	$\frac{1}{3}$	incipient separation
6	−0.3	0	$\frac{1}{3}$	
7	−0.36	0	$\frac{1}{3}$	incipient separation
8	0	0	$\frac{1}{3}$, 0	zero pressure gradient
9	0	0.5	$\frac{1}{3}$, 0	zero pressure gradient

Table 2 Integral method

Case	$\hat{\beta}$	g_w	k_1	Remark
1I	−0.2	0.6	$\frac{1}{3}$	$\tilde{m} = 0.99$ (const)
2I	−0.24	0.6	$\frac{1}{3}$	$\tilde{m} = 0.99$ (const)

Discussion of Results

Cases for which solutions were obtained are listed in Tables 1 and 2. In addition, the integral method was applied to a specific axisymmetric body consisting of a conical forebody and an afterbody with constant curvature turning. The boundary-layer characteristics were calculated on the windward side of this body at angles of attack of 0°, 0.5°, 1°, 2° for flight conditions of $M_\infty = 20$ and 154,000 ft alt. A discussion of the results follows.

For similar solutions, the profiles of the cross-flow velocity function φ_0' and the perturbation velocity and enthalpy profiles, f_1' and g_1, are shown in Figs. 2–4. Examination of these figures indicates that the cross-flow velocity gradient in the boundary layer is sensitive to the wall temperature as well as to the streamwise pressure gradient. In fact, the wall temperature effect may exceed in importance the effect of pressure gradient as indicated by examination of cases 1, 3, 5, and 7. Here, as the values of g_w are increased from 0 to 2.0, while the absolute value of pressure gradient parameter $|\hat{\beta}|$ is simultaneously decreased from 0.360 to 0.1295, the maximum values of φ_0' are greatly increased. On the contrary, the perturbation streamwise velocity profiles, shown in Figs. 3a and 3b, indicate that f_1' is controlled by the pressure gradient for cold walls and for walls with moderate heating, whereas for larger values of g_w, the profiles of f_1' become strongly dependent on the wall temperature, and less dependent on the adverse pressure gradient. These effects can clearly be attributed to the lower boundary-layer densities associated with increasing wall temperature. Similar observations

†† Three first-order nonlinear ordinary differential equations result from a first integration of Eqs. (36–38) after substituting the assumed profiles given by (39).

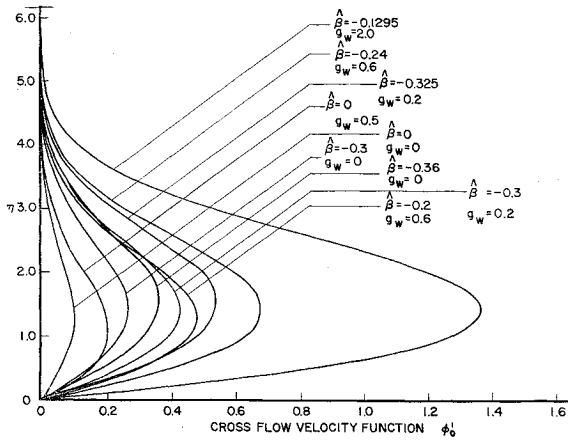

Fig. 2 Cross-flow velocity function profiles.

may be made with regard to the perturbation enthalpy profiles shown in Figs. 4a and 4b.

Figure 5 presents profiles of $f' \cong f_0' + \hat{\alpha} f_1'$, the streamwise velocity profile, for selected values of the cross-flow velocity gradient parameter, $\hat{\alpha}$. In each case, the results are compared to the zero-cross-flow result of Ref. 16, denoted here by $\hat{\alpha} = 0$. Referring to the profiles of f' as shown, it can be seen that, for given wall temperatures, small values of $\hat{\alpha}$ are extremely effective in increasing the streamwise velocity in the boundary layer and in reducing boundary-layer thickness for cases where the layer is experiencing high adverse pressure gradients. As the gradient becomes less severe, the amount of cross-flow, as measured by $\hat{\alpha}$, required to alter the layer increases rapidly. An analogous behavior is observed with respect to the wall temperature condition; as

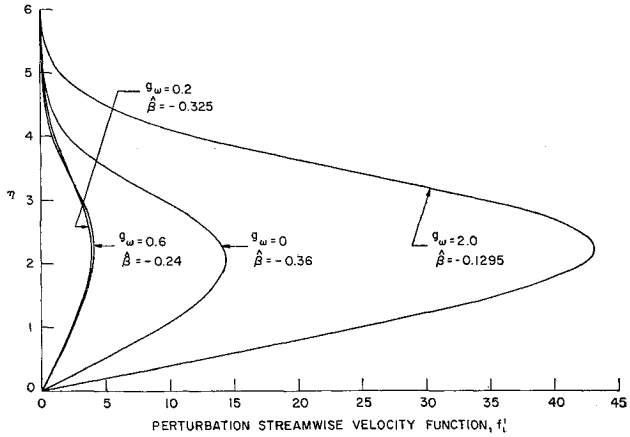

a)

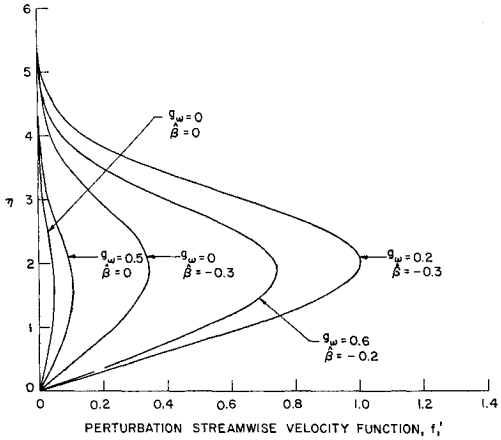

b)

Fig. 3 Perturbation streamwise velocity profiles.

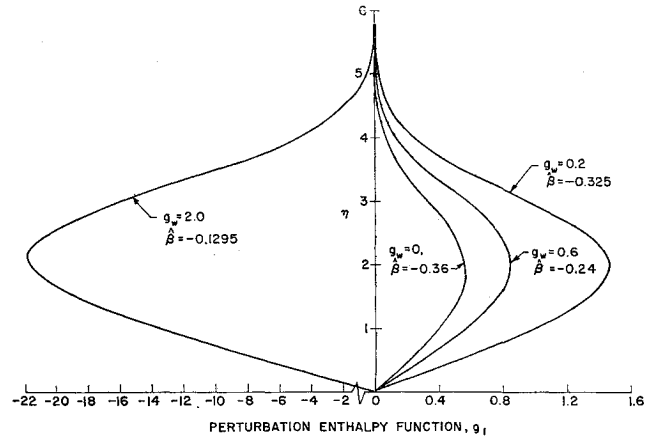

a)

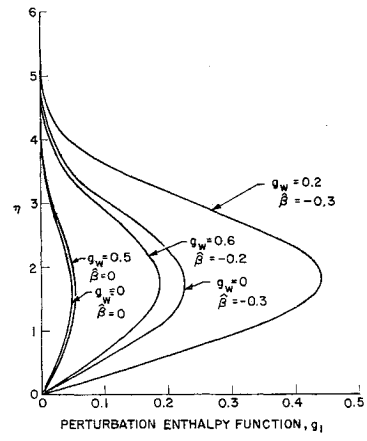

b)

Fig. 4 Perturbation enthalpy function profiles.

the wall is heated to higher values of g_w, smaller cross-flows are required to produce larger alterations of the layer. The effect of cross-flow is small on the enthalpy profiles independent of pressure gradient for cold wall conditions. As g_w increases, however, the effect of cross-flow is to increase the heat transfer to the body.

The specific cases of $\hat{\beta} = 0$ presented in Fig. 5 were chosen to correspond to the results of Reshotko[14] and Moore.[24] Unfortunately, a direct comparison is not possible since, in the present work, the similar solutions were obtained for $\tilde{m} \to 1$, the hypersonic case, whereas those of Reshotko are limited to values of $\tilde{m}$ considerably smaller. However, if the results of Reshotko are roughly extrapolated to conditions of $\tilde{m} \to 1$, then it can be seen that both methods produce essentially the same results for this degenerate case. Moore's results are limited to supersonic flows, thereby precluding direct comparison.

The effect of cross-flow on wall shear is shown in Fig. 6 for small cross-flows. For comparison purposes, calculations were also made using the integral method for $g_w = 0.6$ and for two different pressure gradients. A value of $\tilde{m} = 0.99$ was chosen for the integral method. The results indicate that, for small values of $\hat{\alpha}$, the linearized similar solutions predict wall shears lower than those predicted by the integral method. Two important points should be noted. The first is that both methods predict an increase in wall shear (thereby implying reduced boundary-layer thickness and decreased susceptibility to separation) with increasing cross-flow. The second point is that the linearized method predicts a greater sensitivity to cross-flow for layers approaching separation, whereas the integral method does not exhibit this sensitivity.

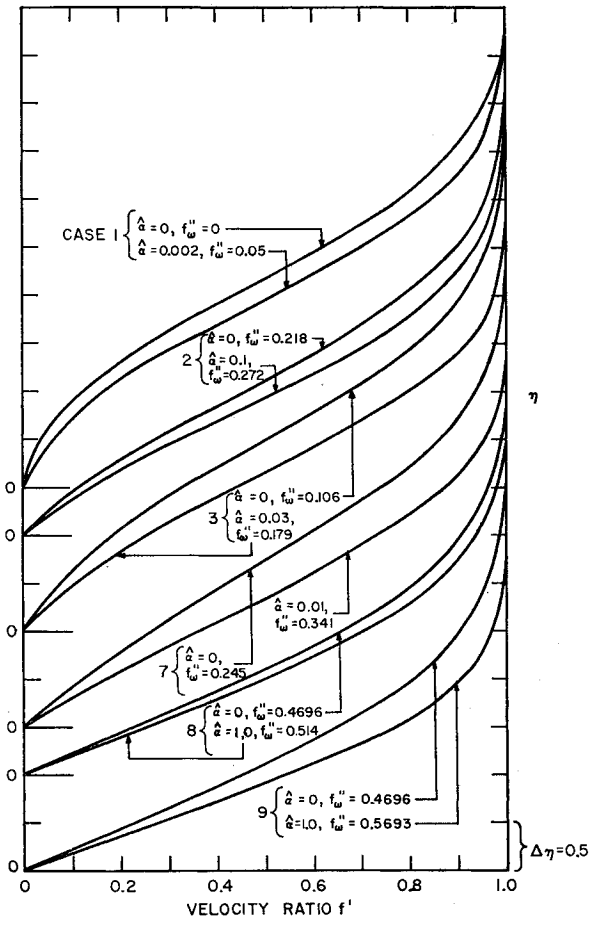

Fig. 5 Streamwise velocity profiles.

Finally, the integral method was applied to the windward side of the axisymmetric body‡‡ shown in Fig. 7 for flight conditions of $M_\infty = 20$ at 154,000 ft alt; $g_w = 0.2$ for angles of attack of 0°, 0.5°, 1°, and 2°. The body consisted of a cone of 5.8° semiapex angle for two-thirds of its length followed by a constant radius of curvature turnover for the remaining one-third of its length for an additional 5.8°.

The magnitude of cross-flow parameter, $\hat{\alpha}$, predicted by an inviscid flow analysis (using Newtonian methods and

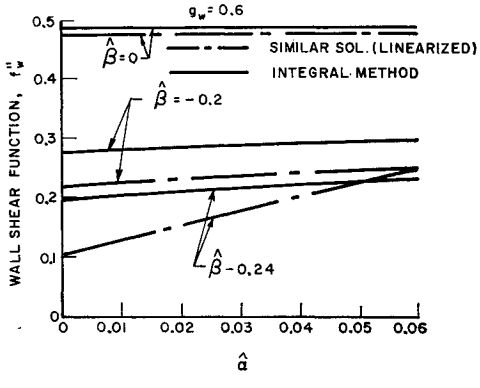

Fig. 6 Effect of cross-flow on wall shear in adverse gradients.

‡‡ It is recognized that the flow on the leeward side of such a body will behave quite differently; this feature has been discussed in Ref. 1 and again in Ref. 15. In the present application, the windward side of a lifting axisymmetric body is being considered only to provide a suitable three-dimensional flow field; the results are indicative of those to be expected for bodies wherein localized three-dimensional outflows can be introduced and are not intended to have direct applicability to axisymmetric inlets or to the entire perimeter of nonaxisymmetric bodies.

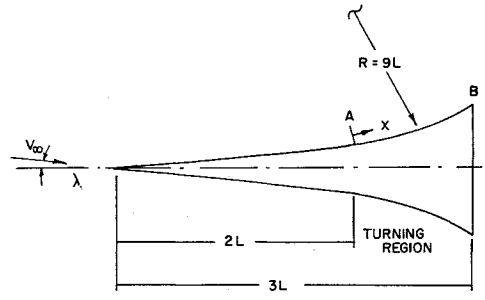

Fig. 7 Axisymmetric body analyzed.

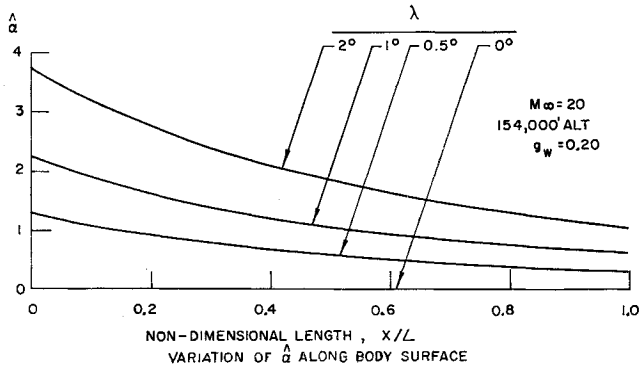

Fig. 8 Variation of $\hat{\alpha}$ along body surface.

described in detail in Ref. 23) is plotted in Fig. 8 as a function of length from the beginning of the turning region for each of the angles of attack considered. It can be seen that, for these stream and body conditions, small angles of attack produce significantly large cross-flows, implying that the validity of the linearized cross-flow analysis is greatly restricted with respect to angle of attack.

The results for the illustrative body are presented in Fig. 9 for two body stations, one at the beginning of the turn and one at the end of turning. Indications are that the cross-flow engendered by angle of attack increased the wall shear and decreased the boundary-layer thickness significantly while increasing the wall heating a somewhat smaller amount at the final station. It should be pointed out that the body chosen for analysis was one in which the flow for $\lambda = 0$ is far from separation, as indicated by the high value of f_w'' shown in Fig. 9. This choice plus the relatively small value of g_w tends to reduce the efficacy of cross-flow in altering the boundary-layer characteristics as noted in the previous discussion. Nevertheless, the anticipated beneficial effects of cross-flow are noted. It is expected that considerably larger

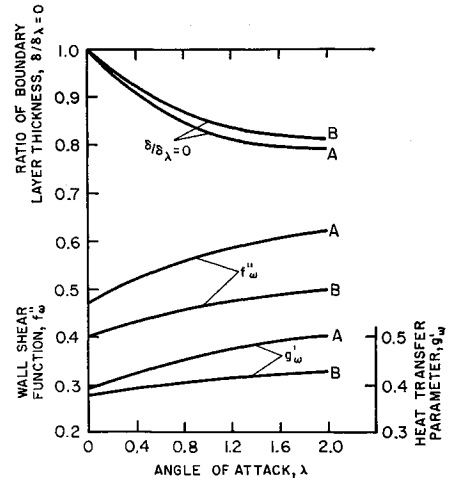

Fig. 9 Effect of angle of attack on wall shear, wall heating, and boundary-layer thickness in turning region.

effects would be observed for a body with a more severe adverse pressure gradient.

Conclusions

Two approaches to the analysis of laminar boundary layers in the plane of symmetry of hypersonic flows with adverse pressure gradients and heat transfer have been employed. The first is based on the concept of similar flows; the second is an integral method useful for both similar and nonsimilar flows.

The analysis of similar flows leads to the usual restrictions that arise for similar flows without cross-flow and to additional restrictions associated with the three-dimensionality. A linearization procedure is followed to describe weak three-dimensional effects. Solutions to the linearized problem imply a significant three-dimensional effect, both with respect to thinning the boundary layer and with respect to delaying separation.

The integral method as developed in this report employs the similarity variables. Thus, the resulting boundary-layer characteristics can be interpreted readily in terms of both similar and nonsimilar flows. When applied to similar flows and compared with the linearized results, this method indicates that, for the flows nearing separation, the linearized method shows a greater sensitivity to cross-flow. Finally, the integral method, when applied to a practical inlet compression surface, demonstrates the beneficial influence of three-dimensionality on the characteristics of the boundary layer on such surfaces.

The results of this investigation indicate the limitations of each method and suggest that extensions of both methods used are in order. With regard to the similar solutions, the next step will be to attempt a numerical solution of the full nonlinear system in order to remove the restriction of small cross-flow associated with the present linearized method. A further refinement of the integral method employing a multiple integral approach, due to Tani,[22] is warranted in view of the inaccuracies associated with adverse pressure gradients. As a final step in this program, the present concepts and the suggested advancements should be applied to flows with turbulent boundary layers.

References

[1] Moore, F. K., "Three dimensional boundary layer theory," *Advances in Applied Mechanics* (Academic Press, New York, 1956), Vol. IV, pp. 160–224.

[2] Cooke, J. C. and Hall, M. G., "Boundary layer in three dimensions," AGARD Rept. 273 (April 1960).

[3] Wilkinson, J., "Some examples of three-dimensional effects in boundary layer flow," Aeronaut. Quart. **V**, 73 (1954).

[4] Moore, F. K., "The unsteady laminar boundary layer of a wedge and a related three-dimensional problem," *Proceedings of the 1957 Heat Transfer and Fluid Mechanics Institute* (Stanford University Press, Stanford, Calif., 1957).

[5] Johnston, J. P., "The turbulent boundary layer at a plane of symmetry in a three-dimensional flow," Am. Soc. Mech. Engrs. Paper 59-Hyd-6 (1959).

[6] Sears, W. R., "The boundary layer of yawed cylinders," J. Aeronaut. Sci. **15**, 49–52 (1948).

[7] Wild, J. M., "The boundary layer of yawed infinite wings," J. Aeronaut. Sci. **16**, 41–45 (1949).

[8] Cooke, J. C., "The boundary layer of a class of infinite yawed cylinders," Proc. Cambridge Phil. Soc. **46**, 645–648 (1950).

[9] Young, A. D. and Booth, T. B., "The profile drag of yawed wings of infinite span," College of Aeronautics, Cranfield, Rept. 38; also Aeronaut. Quart. **3**, 211–229 (1951).

[10] Altman, J. M. and Hayter, N. L. F., "A comparison of the turbulent boundary layer growth on an unswept and a swept wing," NACA TN 2500 (1951).

[11] Lees, L., "Laminar heat transfer over blunt-nosed bodies at hypersonic flight speeds," Jet Propulsion **26**, 259–269 (1956).

[12] Hayes, W. D. and Probstein, R. F., *Hypersonic Flow Theory* (Academic Press, New York, 1959), pp. 284–332.

[13] Vaglio-Laurin, R., "Laminar heat transfer on three-dimensional blunt nosed bodies in hypersonic flow," ARS J. **29**, 123–129 (1959).

[14] Reshotko, E., "Laminar boundary layer with heat transfer on a cone at angle of attack in a supersonic stream," NACA TN 4152 (December 1957).

[15] Libby, P. A. and Fox, H., "Theoretical analyses of some three-dimensional boundary layers with particular applicability to hypersonic inlets, Part II, Laminar flow along a centerline of symmetry," General Applied Science Labs., Inc., Rept. 304 (September 1962).

[16] Cohen, C. B. and Reshotko, E., "Similar solutions for the compressible laminar boundary layer with heat transfer and pressure gradients," NACA Rept. 1293 (1956).

[17] Chapman, D. R. and Rubesin, M. R., "Temperature and velocity profiles in the comprehensible laminar boundary layer with arbitrary distribution of surface temperature," J. Aeronaut. Sci. **16**, 547–565 (1949).

[18] Fox, H. and Libby, P. A., "Helium injection into the boundary layer at an axisymmetric stagnation point," J. Aeronaut. Sci. **29**, 921–935 (1962); also Polytechnic Inst. Brooklyn, PIBAL Rept. 714, ARL 139 (September 1961).

[19] Wilson, R. E., "Real-gas laminar boundary layer skin friction and heat transfer," J. Aerospace Sci. **29**, 640 (1962).

[20] Ashkenas, H. and Riddell, F. R., "Investigation of the turbulent boundary layer on a yawed flat plate," NACA TN 3383 (April 1955).

[21] Hayes, W. D., "On laminar boundary layers with heat transfer," Jet Propulsion **26**, 270–274 (1956).

[22] Tani, I., "On the approximate solution of the laminar boundary layer equations," J. Aeronaut. Sci. **21**, 487–495, 504 (1954).

[23] Sanator, R. J. and De Carlo, J., "Three-dimensional laminar boundary layer analysis of hypersonic inlet flows near a plane of symmetry," Republic Aviation Corp. Rept. RAC 1310(AVD-1024) (April 1963).

[24] Moore, F. K., "Laminar boundary layer on a circular cone in supersonic flow at a small angle of attack," NACA TN 2521 (October 1951).